

Original Research

# Photocatalytic Removal of Azo Dyes Using a CNT Doped ZnO/Fe<sub>2</sub>O<sub>3</sub> Catalyst

Waheed Tariq<sup>1</sup>, Ch. Arslan<sup>1\*</sup>, Sohali Ali Naqvi<sup>3</sup>, Muhammad Abdullah<sup>3</sup>,  
Abdul Nasir<sup>1</sup>, Syed Hamza Gillani<sup>1</sup>, Abdul Ghafoor<sup>2</sup>, Asma Sattar<sup>1</sup>, Haroon Rashid<sup>1</sup>,  
Muhammad Yamin<sup>2</sup>

<sup>1</sup>Department of Structures and Environmental Engineering, University of Agriculture, Faisalabad, Pakistan

<sup>2</sup>Department of Farm Machinery and Power, University of Agriculture, Faisalabad, Pakistan

<sup>3</sup>World Wide Fund Nature - Pakistan

Received: 16 September 2020

Accepted: 18 December 2020

## Abstract

Textile dyes especially azo dyes are the prime pollutants in wastewater due to the presence of complex azo bond (–N=N–). Many conventional methods such as physicochemical, mechanical and biochemical were employed recently for removal of these organic pollutants. These methods have not been proved to be so efficient. Photocatalysis, a latest physio-chemical methods is employed currently. Present work investigated the synthesis of a Carbon Nano Tubes (CNT's) doped ZnO/Fe<sub>2</sub>O<sub>3</sub> catalyst by microwave-assisted sol-gel method. Removal efficiency of the synthesized catalyst was observed through removal of two azo dyes direct orange-26 and acid red-151 for different concentrations. The prepared ternary nano-hybrid was characterized by X-ray diffractometry (XRD), scanning electron microscopy (SEM) and Energy Dispersive Spectroscopy (EDS). The average crystalline size of the catalyst was calculated as 8.47nm by using data from XRD analysis. SEM images revealed the formation of nano-flakes of catalyst. And results of EDS investigation publicized that the distribution of all the atoms of Zn, Fe, O and C is homogeneous throughout the catalyst. Percentage removal by synthesized catalyst for direct orange-26 and acid red-151 was determined as 58.8% and 72.7% respectively without adding oxidant. After adding oxidant the percentage removal increases to 70.6% for direct orange-26 and 85.2% for acid red-151. The effect of pH, time and oxidant dose were optimized by developing relationships between these variables using central composite design (CCD) in response surface methodology (RSM). The results of RSM analysis show prepared catalyst performs best in acidic conditions at pH of 3 and irradiation time of 2.7 hours for acid red-151 and at pH of 5 and irradiation time of 3.8 hours for direct orange-26.

**Keywords:** CNT's doped ZnO/Fe<sub>2</sub>O<sub>3</sub> catalyst, RSM, azo dye, Photocatalysis, wastewater treatment

## Introduction

The discharge of industrial effluents into the environment is a very concerning issue. The wastewater from textile industries is a major hazard for the aquatic environment. Some dyes are released into the environment which leads to detrimental effects [1]. These dyes are the persistent pollutants that have a tendency to be bio-accumulate in living organisms leading to numerous diseases and disorders. [2, 3]. Almost 0.7 million tons of various combinations of coloring from commercially available 0.1 million dyes are synthesized each year. The leftover dye mixture after the completion of concerned process, is released into the environment [4, 5]. Every year almost 2, 80,000 tons of textile dyes are discharged into the environment through industrial effluents globally [6].

Azo dyes are the frequently used agents in textile sector as these accommodate 60% out of total dyes being employed in textile industries [7]. Azo dyes are characterized by the existence of the azo group (i.e.  $-N=N-$ ) in their molecular structure. Due to large molecular size, chemical nature and structural diversity azo dyes have advanced optical and thermal properties [8]. Moreover, stable amines are formed due to the existence of the reductive cleavage of azo linkages [9]. Being very stable, azo dyes are resistant to degradation and micro-organisms, so it is undesirable to be present in water streams [10].

Different conventional methods e.g. ultrafiltration, reverse osmosis, adsorption by activated carbon membrane separation, bioaccumulation and ion exchange [8, 11, 12] have been adopted for the decontamination of pollutants from wastewater. Partial degradation, high cost, generation of hazardous solid waste, and high stability are prime disadvantages of these methods, specifically for dye removal [13]. Consequently, there is a necessity for economical and more effective methods of treating textile effluents which consumes minimum energy and chemicals. Advanced oxidation processes (AOP) especially heterogeneous photocatalysis has been adopted successfully for the removal of dyes and other toxic compounds by total conversion of these compounds into non-toxic species [14]. AOPs seeking high consideration of scientific community as by publication of huge no. of important and applied research [15]. As a result of wide research, it can be conclude these methods are effective and environmental-friendly techniques. The redox technique not only enable decolonization but decay of dye on employing various types of oxidizing agents. Alteration in the chemical building of POPS like dyes: way towards meeting with these oxidizing agents leading to make them susceptible to degradation [16].

There are numerous catalysts ( $TiO_2$ ,  $ZnO$ ,  $Fe_2O_3$  etc.) and their composites (i.e.  $ZnO/Fe_2O_3$ ,  $ZnO/\alpha-Fe_2O_3$ , etc.) have been adopted for remediation of wastewater

[17, 18]. Previously researchers utilized these catalysts for simple and basic dyes that are easily degraded. Very rare reports are found on photocatalytic removal of azo dyes. Composites of catalysts present high removal rates of highly stable pollutants as compared to single catalysts.

Pure  $CoFe_2O_4$  and  $CoFe_2O_4/Ag_2O$  were utilized to determine the visible light photocatalytic degradation of Direct Orange 26.  $Ag_2O$ -modified  $CoFe_2O_4$  exhibited 40% higher photocatalytic activity than the unmodified one [1]. While the removal rates of Methylene Orange were found to be 76%, 85% and 97.5% with the application of  $ZnO$ ,  $ZnO/ZnS$  and  $ZnO/ZnS/\alpha-Fe_2O_3$  nanocomposites respectively [19]. Synthesized  $Fe_2O_3/ZnO$  exhibits 98% degradation of Methylene Orange as compared to 80% degradation by simple  $ZnO$  catalyst [20, 21].  $ZnO/Fe_2O_3$  NT shows 81.8% removal of MB dye under UV light irradiation that is 20% higher than the removal by bare  $ZnO$  Nano rods [17].  $\alpha-Fe_2O_3/ZnO$  nanocomposite (NC) were synthesized and applied for removal of MB. Synthesized catalyst exhibited 65% removal of MB in 320 minutes that is higher than bare  $ZnO$  and  $Fe_2O_3$  that shows 12% and 20.9% removal respectively [22]. Recently Carbon Nano Tubes (CNT's) have been utilized with the composites of different catalysts. The catalyst  $ZnO/Ag/CNT$  presented 81% removal of MB as compared to 43% by  $ZnO/Ag$ , 19% by pure  $ZnO$  and 16% by bare CNT [23]. It explored that previously reported catalyst are not so much efficient and also takes a lot of time to fully remove dyes from wastewater. So there is need to improve the efficiency of these catalyst by using different composites of these catalysts.

For resolving the mentioned issues and devising a proper strategy, current study explored the removal of azo dyes by developing an effective novel catalyst by simple and cost effective method. Scientific approach was used for the removal of azo dyes to destabilize the textile dyes in synthetic solutions. A new CNT doped  $ZnO/Fe_2O_3$  catalyst was synthesized and its photocatalytic performance was measured by removal of two azo dyes direct orange-26 and acid red-151.

## Materials and Methods

### Preparation of CNT Doped $ZnO/Fe_2O_3$ Catalyst

Catalyst of  $ZnO/Fe_2O_3$  was prepared using microwave assisted Sol-gel method with some modification stated by [24]. The prepared catalyst was filtered and pH was adjusted to 7 by washing several times with distilled water during filtration. Then hydrophilic CNT's were added in already prepared  $ZnO/Fe_2O_3$  catalyst and solution was prepared by adding 20 mL distilled water. After stirring and sonication the solution was filtered through filtration assembly and then filtrate was oven dried to remove moisture.

## Characterization Analysis

### Crystalline Structure of Catalyst

The XRD pattern of the sample (catalyst) was recorded by using Cu K $\alpha$  radiation at 1.5418 Å of  $\lambda$  value with diffractometer at 0.05 per minute scanning rate for  $2\theta$  values ranging from 10.130°–70.139°. From the XRD pattern, average crystallite size is estimated by Scherrer formula (Equation 1).

$$D = \frac{k\lambda}{\beta \cos \theta} \quad (1)$$

Where, D = crystallite sizes,  $\beta$  = FWHM = Full width half maximum value,  $\lambda$  = X-ray wavelength, k = scale factor k value depends on the grains shape, and is always close to 1 [25-27].

### Surface Topography and Composition

Scanning Electron Microscopy (SEM) is powerful microscopic techniques to look into material chemistry at micro and Nano levels. SEM focuses an electron beam and scans over a surface to generate an image. Electrons of the beam produces various signals by interacting with sample, then these signals are processed to acquire information about the composition of sample and surface topography. EDS determines the composition of catalyst. Therefore our synthesized catalyst was analyzed using SEM/EDS for the revelation of the composition and topographical analysis of the catalyst.

### Pollutants Study

Two azo dyes employed in this study are very complicated in terms of structures. Direct orange-26 has molecular weight of 756.67 g/mol,  $\lambda_{\max}$  of 493 and molecular formula of C<sub>33</sub>H<sub>22</sub>N<sub>6</sub>Na<sub>2</sub>O<sub>9</sub>S<sub>2</sub> [28]. The molecular weight of acid red-151 is 454.44 g/mol [29] and molecular formula is C<sub>22</sub>H<sub>15</sub>N<sub>4</sub>NaO<sub>4</sub>S, having maximum absorbance in spectrophotometric analysis at  $\lambda_{\max}$  = 512 [30]. Molecular structure of direct orange-26 and acid red-151 is shown in Fig. 1.

### Response Surface Methodology (RSM)

The main idea of RSM is to find an optimal response by a sequence of designed experiments. So, RSM was

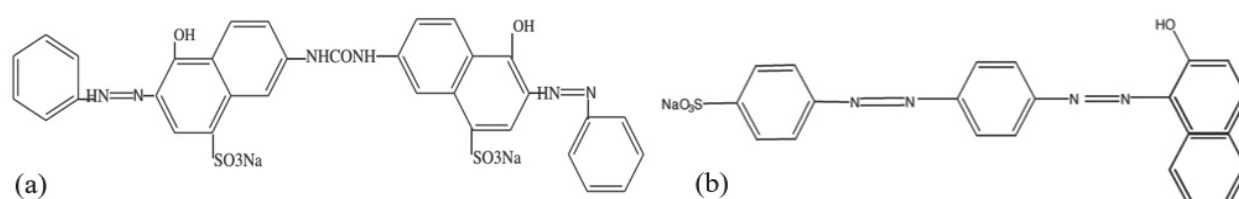


Fig. 1. Complex molecular structure of a) Direct Orange-26 [28] b) Acid red-151 [31].

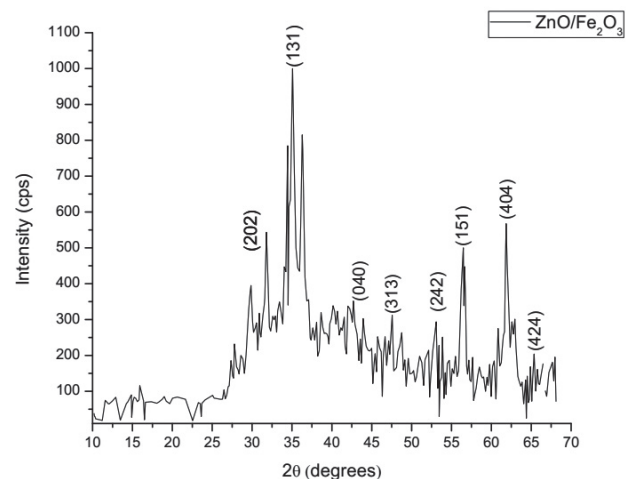


Fig. 2. XRD spectra of ZnO/Fe<sub>2</sub>O<sub>3</sub> Catalyst with miller indexes of major peaks.

used to optimize the effect of three parameters (pH, time and oxidant dose). These parameters were designated as independent variables, while the percentage removal of dyes was designated as the dependent response variable in the central catalyst design (CSD). The response of all designated experiments were recorded and analyzed by software to generate contour maps and 3D surfaces.

### Experimental Setup

Photocatalytic removal efficiency of prepared catalyst was measured with a series of experiments. Reaction kinetics experiments were conducted on dye solutions of different concentrations (5 ppm, 10 ppm, 20 ppm, 40 ppm, 80 ppm) to study the behavior of removal of dyes with the increasing irradiance time. To analyze the effect of oxidant on removal process reaction kinetics experiments were conducted with and without adding oxidant (H<sub>2</sub>O<sub>2</sub>). The experiment was allowed to run for 240 minutes in total. The percentage reduction of dye concentration was measured according to the following Equation (2):

$$\text{Percentage dye degradation} = \frac{A_{in} - A_f}{A_{in}} \times 100 \quad (2)$$

Where,  $A_{in}$  = initial dye concentration (ppm) and  $A_f$  = Final dye concentration (ppm).



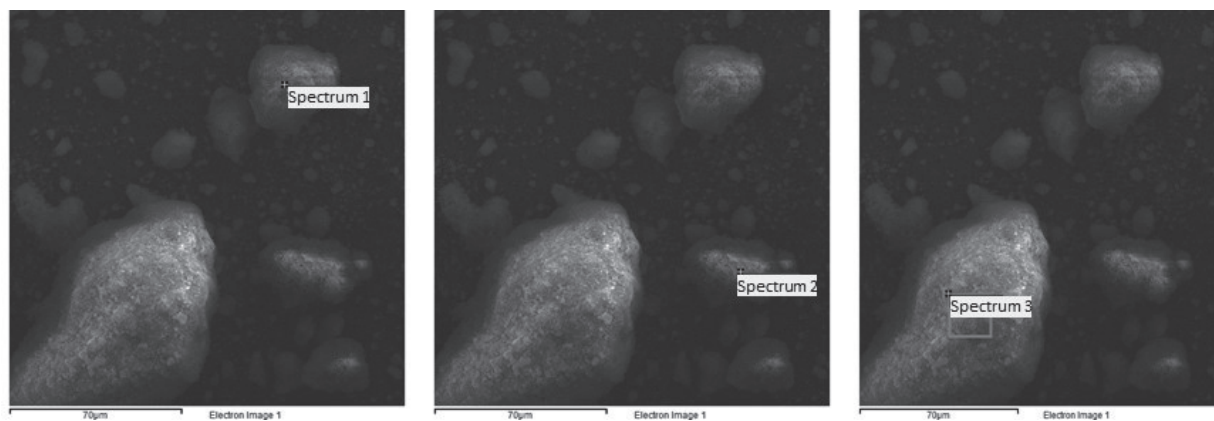


Fig. 4. EDS element distribution images analyzed as Spectrum 1 a), Spectrum 2 b) and Spectrum 3 c).

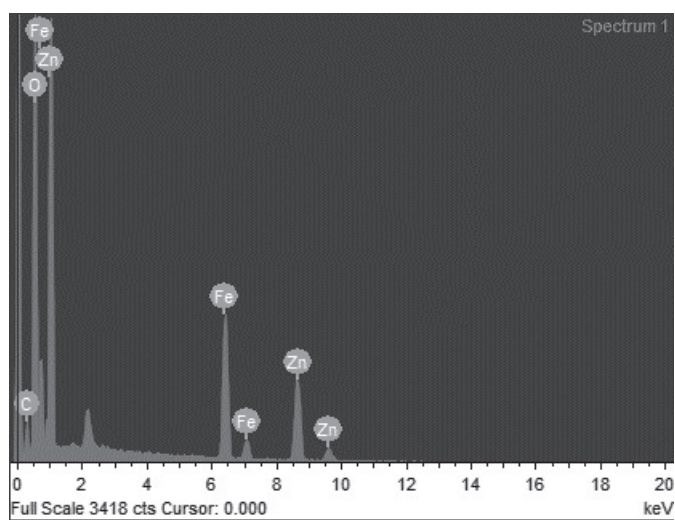


Fig. 5. Energy peaks of all elements present in catalyst examined through EDS.

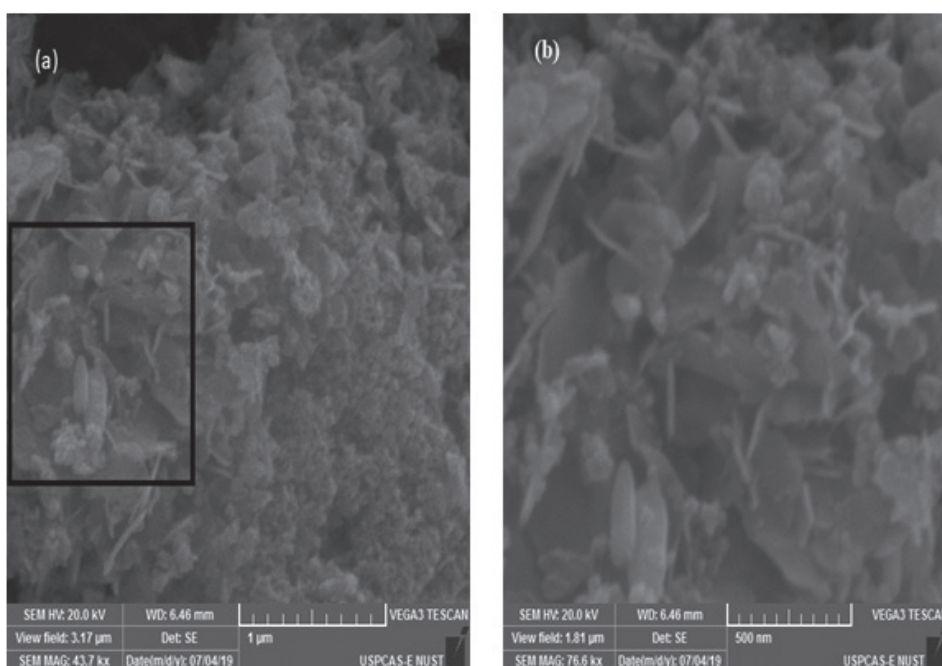


Fig. 6. SEM Image of ZnO/Fe<sub>2</sub>O<sub>3</sub>/CNT Catalyst at 1 µm a) and is zoom in at square area up to 500 nm b).

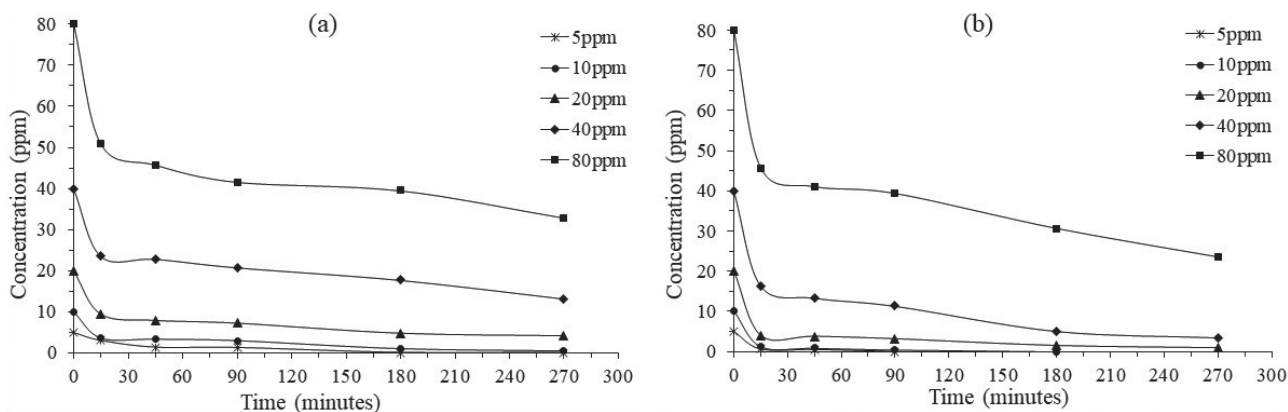


Fig. 7. Removal behavior of Direct Orange-26 a) without oxidant b) after adding oxidant.

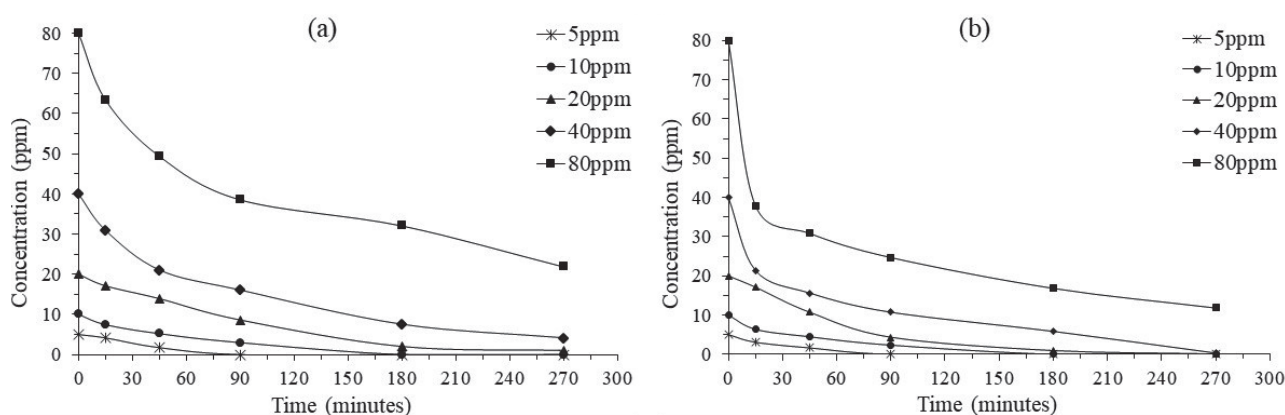


Fig. 8. Removal behavior of Acid Red-151 a) without oxidant b) after adding oxidant.

slowly at the start and maximum removal occurs in first 30 minutes. The removal curves show that the catalyst still has potential for further removal of dyes. It was observed that by adding oxidant removal occurs more quickly as well as gives better results in terms of percentage removal.

The removal behavior of direct orange-26 dye by catalyst without adding oxidant is shown in Fig 7a) and Fig. 7b) shows the removal behavior of dye by catalyst with oxidant (4 mL). It was observed that by adding oxidant removal occurs more quickly as well as gives better results in terms of percentage removal. While discussing the highest percentage removal based on 80ppm initial concentration, it is 58.8 % without oxidant and it increases to 70.6 % by adding oxidant for direct orange-26. Similarly experiment was repeated with Acid Red-151 dye solutions with the same conditions. Similar removal trend was observed for this dye with some high removal rates. Maximum removal (72.7%) for 80 ppm solution was observed without addition of oxidant and dye removal increases to 85.2% for 80 ppm solution after the addition of oxidant. Fig. 8a) shows the removal behavior of dye acid Red-151 by applied catalyst (CNT's doped ZnO/Fe<sub>2</sub>O<sub>3</sub>) without adding oxidant. And Fig. 8b) shows the removal behavior of dye by applied catalyst with oxidant (4 mL).

### Optimization of Process Parameters and Data Analysis by Response Surface Methodology (RSM)

The adequacy and significance of multiple regression model was justified by the analysis of variance (ANOVA) using central composite design (CCD) under Response Surface Methodology (RSM). After running experiments as described in previous sections 3D response surface and contour maps were plotted for both the dyes.

#### RSM Analysis of Direct Orange-26

Analysis of variance reveal that developed model is significant as indicated by F-value of 11.35, p-value of 0.0004 indicated that there are only a 0.04 percent chances "F-value of Model" could be larger than 11.35, that may be due to noise. F-value of 3.59 for Lack of Fit refers to insignificance of Lack of Fit test attributed to adequacy of designed model. p-value of 0.118 indicates that there are 11.81 percent chances of chance that a "Lack of Fit " could be significant that is due to noise. Moreover the effect of pH is most significant as compared to other independent variables. The quadratic effect of independent variables is not discussed here. The coefficient of variation (C.V) was calculated

as 9.61% that is attributed towards the validity of the data obtained during experiment because it is below 10% that is recommended for laboratory experiments. All the calculations of model are based on Equation (3).

$$\begin{aligned} \text{Percentage Removal} = & 90.40 - 17.17A + 3.96 B \\ & - 2.35C + 2.65AB - 0.55AC + 1.57 BC \\ & - 8.69A^2 - 3.49B^2 - 5.44C^2 \end{aligned} \quad (3)$$

Where,

Percentage Removal = Dependent variable

90.40 = intercept

A = 1<sup>st</sup> independent variable (pH)

B = 2<sup>nd</sup> Independent variable (Time of irradiation)

C = 3<sup>rd</sup> Independent variable (Oxidant Dose)

And all other constant values are regression coefficients.

Fig. 9a) shows 3D surface of % age dye removal as a function of time and pH and 9b) shows the contour mapping of designated independent variables pH and time which describes that removal of direct orange-26 dye increases as time increases and decreases with increases pH. These conditions were optimized at pH = 5 and irradiance time of 3.5 hours as that is maximum percentage removal (91.5%) in response to these two independent variables. Similarly, the response of dependent variable against time and oxidant dose is represented in Fig. 9c) and 9d), which describes that removal was best obtained (88.61%) after 3.5 hours and at oxidant amount of 4 mL and explains that

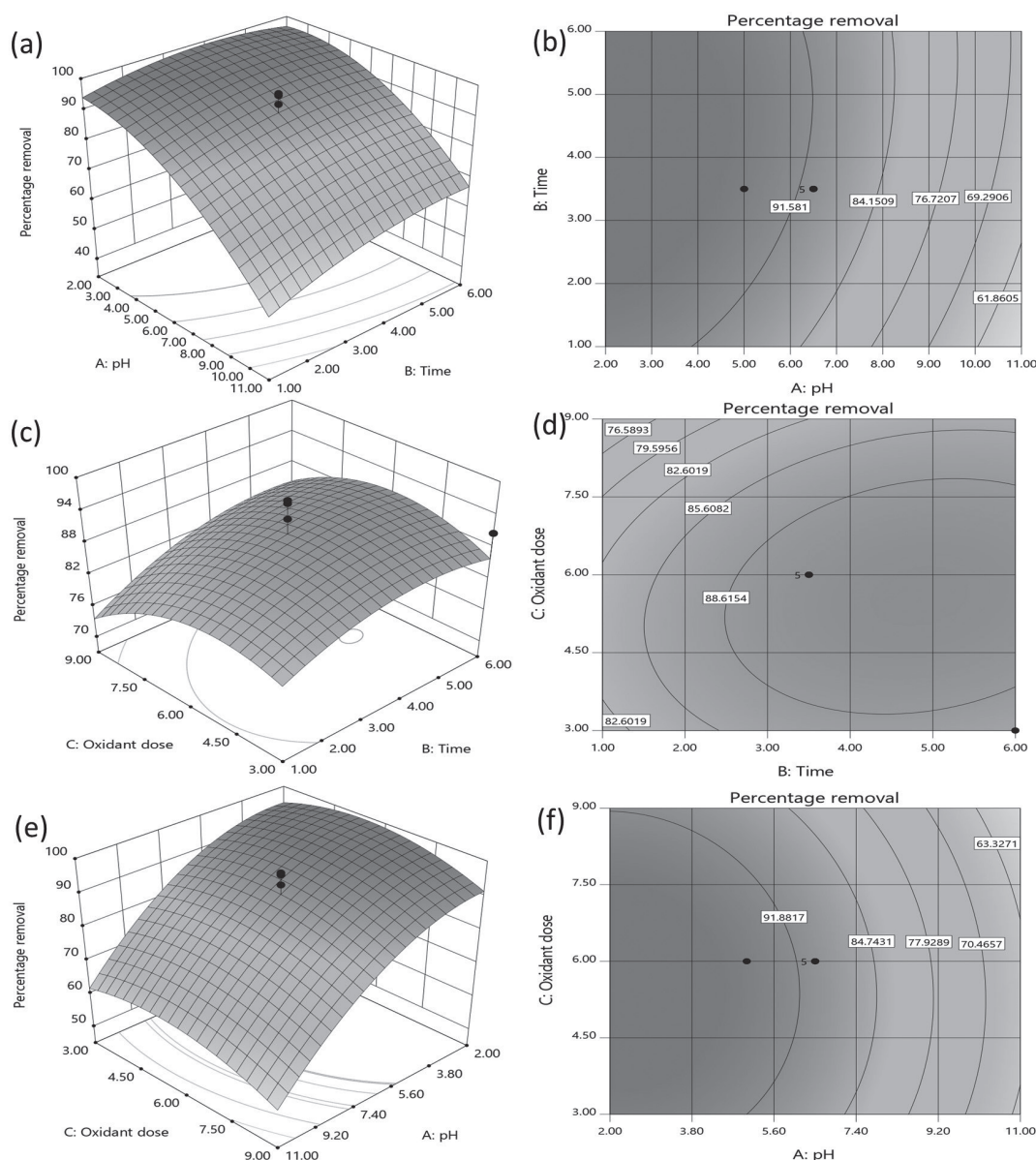


Fig. 9. Optimization responses of the designated parameters for direct orange-26 a) 3D Response surface and b) contour map of percentage removal (%) as a function of A:pH and B:time (hours), c) 3D Response surface and d) contour map of percentage removal (%) as a function of B:time (hours) and C:Oxidant dose (mL), e) 3D Response surface and b) contour map of percentage removal (%) as a function of A:pH and C:Oxidant dose (mL).

by increasing oxidant dose firstly removal increases and then goes on decreasing. Time has direct effect as by increasing time of irradiance removal goes on increasing.

While discussing the response of dependent variable towards combined effect of pH and oxidant dose, Fig. 9 e) displays 3D surface response image and 9 f) shows contour map which clearly exhibit that the conditions are best optimized at pH of 4 and 4 mL of oxidant dose that is 91.88 % removal occurs at these optimized condition. Removal has decreased dramatically while increasing the pH, and is almost constant as a reaction to the oxidant dose.

RSM Analysis of Acid Red-151

Analysis of variance gives F-value of 5.04 which confirms the significance of the model. p-value of 0.0093 indicates that there are only a 0.93 percent chances that “F-value of Model” could be large that 5.04, that may be due to noise. F-value of 6.06 for Lack of Fit refers to insignificance of Lack of Fit test attributed to adequacy of designed model. p-value of 0.0514 indicates that there are 5.14 percent chances of chance that a “Lack of Fit “ could be significant that is due to noise. Non-significant lack of fit test is presumed as we want the model to fit. Overall pH affected the removal significantly as compared to other factors. The quadratic effect of independent variable is not

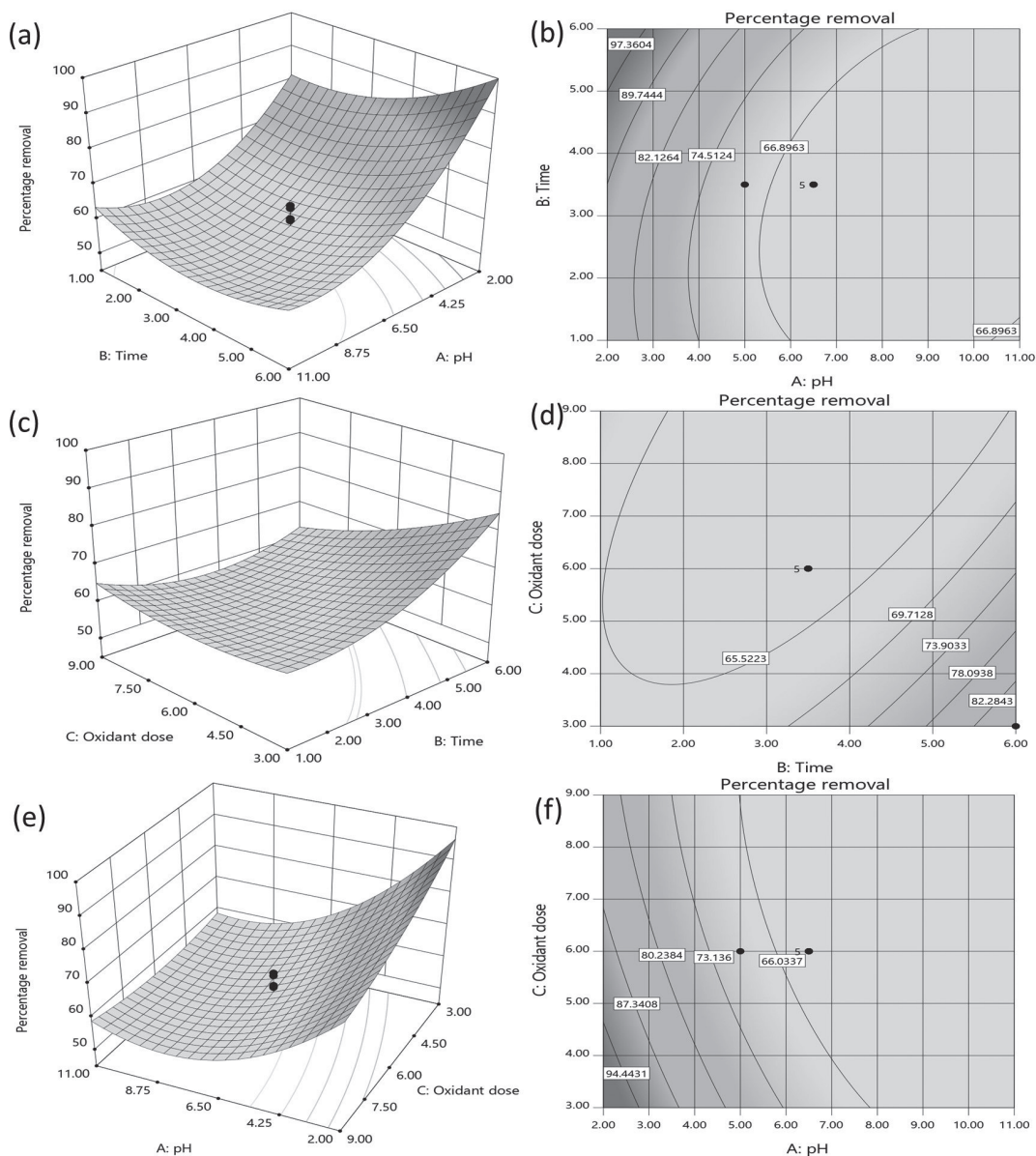


Fig. 10. Optimization responses of the designated parameters for acid red-151 a) 3D Response surface and b) contour map of percentage removal (%) as a function of A:pH and B:time (hours), c) 3D Response surface and d) contour map of percentage removal (%) as a function of B:time (hours) and C:Oxidant dose (mL), e) 3D Response surface and b) contour map of percentage removal (%) as a function of A:pH and C:Oxidant dose (mL).

significantly measured here. The coefficient of variation (C.V) was calculated as 9.91% that is attributed towards the validity of the data obtained during experiment, because it is below 10% that is recommended for laboratory experiments.

$$\begin{aligned} \text{Percentage Removal} = & 63.47 - 14.16A + 3.94B \\ & - 4.56C - 5.12AB + 4.72AC - 5.74BC + 12.08A^2 \\ & + 6.21B^2 + 2.56C^2 \end{aligned} \quad (4)$$

Where,

Percentage Removal = Dependent variable

63.47 = intercept

A = 1<sup>st</sup> independent variable (pH)

B = 2<sup>nd</sup> Independent variable (Time of irradiation)

C = 3<sup>rd</sup> Independent variable (Oxidant Dose)

And all other constant values are regression coefficients.

Fig. 10a) shows 3D surface of % age dye removal as a function of time and pH and 10b) shows the contour mapping and 3D response surface of designated independent variables pH and time that describes that removal of acid red-151 dye increases as time increases and decreases with increases pH as shown in 3D surface. It was observed from the Fig. 15 that pH has reflective effect on dye removal. These conditions were optimized at pH = 2-3 and irradiance time of 3 hours to 3.5 hours that is maximum percentage removal (97.36%) in response to these two independent variables occurs at these conditions and goes on decreasing towards contour with 66.89% removal from pH 6.5 to onwards. As removal is 89.74% after 3.5 hours and pH = 3.2, 82.12% after 3.5 hours and pH value of 4.25.

Similarly, the response of dependent variable against time and oxidant dose is represented in Fig. 10c) in the form of 3D surface map and 10d) as contour map, which describes that removal was best obtained (82.2%) after 3.5 hours and at oxidant amount of 3-4 mL. The effect of oxidant in this relation doesn't seem to be so prominent, as it remains around 70% displayed in 3D surface. However removal increases with increasing time of exposure, as increases from 65% to around 82% with increasing time.

While discussing the response of dependent variable towards combined effect of pH and oxidant dose, Fig. 10 e) presented 3D surface and 10f) shows contour map, which exhibit that the conditions are best optimized at pH of 2-3 and 3-4.5 mL of oxidant dose that is maximum (94.4%) removal occurs at these optimized condition. The effect of pH was still significantly observed, as removal falls from 94% to 60% against increasing pH value. As removal decreases with increasing pH and same trend was observed for oxidant amount as seen in 3D surface. But it is a little straight as compared to pH effect. 3D surface plot shows that removal decreases from 94% to around 86.5%.

Overall it was witnessed that pH mainly influences the percentage removal of dyes under examination.

Maximum removal of under study dyes was examined in acidic conditions, however direct orange-26 best degraded at pH 5 and the value of pH is 3 for acid red-151. It is clear that removal increases as the time of exposure to light increases, but it is not feasible to go for maximum irradiance time, so time is optimized to 3.5 hours for better removal of azo dyes.

## Conclusion

Wastewater generation from textile units is of great concern in this era of industrialization. Dyes being mostly utilized agents in textile sector are causing wear pollution concerns. The synthesized catalyst is a novel catalyst and was found to be effective for the removal of azo dyes from wastewater. All the characterization results of synthesized catalyst confirms that the catalyst was fabricated as desired. All the elements are well distributed in catalyst homogeneously as confirms by EDS results. It was perceived that the efficiency of this dye removal approach was as good for both dyes as it supposed to be. Removal starts in first 15 minutes of catalytic reaction in case of both dyes. But is best optimized b/w 180 to 220 minutes for both dyes. The effect of oxidant was also significant as removal rates were well increased by addition of oxidant (H<sub>2</sub>O<sub>2</sub>). The removal of direct orange-26 is little bit slower because of its difficult structure. The optimal condition from RSM analysis for removal were found to be pH of 5, irradiation time of 220 minutes and oxidant dose of 3.5 mL for direct orange-26, and pH of 3, irradiation time of 180 minutes and oxidant dose of 3 mL were the optimized conditions for acid red-151.

## Acknowledgments

The authors acknowledge the support from Prof. Dr. Ijaz Ahmad Bhatti head of analytical chemistry lab and chairman, department of chemistry, UAF who provided help in different experiments and also thankful to dr. Zuhair S. Khan in-charge of combined lab, U.S.-Pakistan Centre for Advanced Studies in Energy at NUST which provided help for characterization analysis. We are also thankful to WWF for their support.

## Conflict of Interest

The authors declare no conflict of interest.

## References

1. MEHDIPOUR GHAZI M., AZHDARI F. Photocatalytic degradation of textile dye direct orange 26 by using CoFe<sub>2</sub>O<sub>4</sub>/Ag<sub>2</sub>O. *Advances in Environmental Technology*, 2 (2), 77, 2016.

2. EL-HOSINY F., ABDEL-KHALEK M., SELIM K.A., OSAMA I. Physicochemical study of dye removal using electro-coagulation-flotation process: Physicochemical Problems of Mineral Processing, **54** (2), 47, **2018**.
3. SINGH S., BARICK K., BAHADUR, D. Functional oxide nanomaterials and nanocomposites for the removal of heavy metals and dyes. *Nanomaterials and Nanotechnology*, **3**, 3, **2013**.
4. ABDI J., VOSSOUGH M., MAHMOODI N.M., ALEMZADEH I. Synthesis of metal-organic framework hybrid nanocomposites based on GO and CNT with high adsorption capacity for dye removal. *Chemical Engineering Journal*, **326**, 1145, **2017**.
5. RAFATULLAH M., SULAIMAN O., HASHIM R., AHMAD A. Adsorption of methylene blue on low-cost adsorbents: a review. *Journal of hazardous materials*, **177** (1-3), 70, **2010**.
6. GUPTA S., ANNEPU S.K., SUMMUNA B., GUPTA M., NAIR S.A. Role of Mushroom Fungi in Decolourization of Industrial Dyes and Degradation of Agrochemicals. *Biology of Macrofungi*, Springer, 177, **2018**.
7. SIDDIQUE K., RIZWAN M., SHAHID M.J., ALI S., AHMAD R., RIZVI H. Textile wastewater treatment options: a critical review. *Enhancing Cleanup of Environmental Pollutants*. Springer. 183, **2017**.
8. DANESHVAR E., KOUSHA M., KOUTAHZADEH N., SOHRABI M.S., BHATNAGAR A. Biosorption and bioaccumulation studies of acid Orange 7 dye by *Ceratophyllum demersum*. *Environmental Progress & Sustainable Energy*, **32** (2), 285, **2013**.
9. SREEDHARAN V., RAO K.V. Biodegradation of Textile Azo Dyes. *Nanoscience and Biotechnology for Environmental Applications*, Springer International Publishing, 115, **2019**.
10. KONICKI W., ALEKSANDRZAK M., MOSZYŃSKI D., MIJOWSKAE. Adsorption of anionic azo-dyes from aqueous solutions onto graphene oxide: equilibrium, kinetic and thermodynamic studies. *Journal of colloid and interface science*, **496**, 188, **2017**.
11. ESFAHANI M., STRETZ H.A., WELLS M.J. Comparing humic acid and protein fouling on polysulfone ultrafiltration membranes: Adsorption and reversibility. *Journal of Water Process Engineering*, **6**, 83, **2015**.
12. SELVAKUMAR K., BADARINARAYANAN N., UMESH A., EZHILKUMAR P., YUVANASHREE E. Acid dye degradation using electrochemical batch recirculation flow reactor. *J Chem Pharm Sci*, **9**, 308, **2016**.
13. VIKRANT K., GIRI B.S., RAZA N., ROY K., KIM K.-H., RAI B.N., SINGH R.S. Recent advancements in bioremediation of dye: current status and challenges. *Bioresource technology*, **253**, 355, **2018**.
14. MIKLOS D., REMY C., JEKEL M., LINDEN K.G., DREWES J.E., HÜBNER U. Evaluation of advanced oxidation processes for water and wastewater treatment – a critical review. *Water Research*, **139**, 118, **2018**.
15. DA SILVA L.D.M., GOZZI F., SIRÉS I., BRILLAS E., DE OLIVEIRA S.C., JUNIOR A.M. Degradation of 4-aminoantipyrine by electro-oxidation with a boron-doped diamond anode: Optimization by central composite design, oxidation products and toxicity. *Science of The Total Environment*, **631**, 1079, **2018**.
16. ABDEL-HALIM E., AL-DEYAB S.S. One-step bleaching process for cotton fabrics using activated hydrogen peroxide. *Carbohydrate polymers*, **92** (2), 1844, **2013**.
17. HASHIM F.S., ALKAIM A.F., MAHDI S.M., ALKHAYATT A.H.O. Photocatalytic degradation of GRL dye from aqueous solutions in the presence of ZnO/Fe<sub>2</sub>O<sub>3</sub> nanocomposites. *Composites Communications*. **16**, 3, **2019**.
18. AL-MAMUN M., KADER S., ISLAM M., KHAN M. Photocatalytic activity improvement and application of UV-TiO<sub>2</sub> photocatalysis in textile wastewater treatment: a review. *Journal of environmental chemical engineering*. **7**, 5, **2019**.
19. [HITKARI G., SINGH S., PANDEY G. Photoluminescence behavior and visible light photocatalytic activity of ZnO, ZnO/ZnS and ZnO/ZnS/ $\alpha$ -Fe<sub>2</sub>O<sub>3</sub> nanocomposites. *Transactions of Nonferrous Metals Society of China*, **28** (7), 1386, **2018**.
20. PIRHASHEMI M., HABIBI-YANGJEH A., POURAN S.R. Review on the criteria anticipated for the fabrication of highly efficient ZnO-based visible-light-driven photocatalysts. *Journal of industrial and engineering chemistry*, **62**, 1, **2018**.
21. SURYAVANSHI R., MOHITE S., BAGADE A., RAJPURE K. Photoelectrocatalytic activity of spray deposited Fe<sub>2</sub>O<sub>3</sub>/ZnO photoelectrode for degradation of salicylic acid and methyl orange dye under solar radiation. *Materials Science and Engineering: B*, **248**, 114386, **2019**.
22. NORUOZI A., NEZAMZADEH-EJHIEH A. Preparation, characterization, and investigation of the catalytic property of  $\alpha$ -Fe<sub>2</sub>O<sub>3</sub>-ZnO nanoparticles in the photodegradation and mineralization of methylene blue. *Chemical Physics Letters*. **752**, 137587, **2020**.
23. MOHAMMED M.K. Carbon nanotubes loaded ZnO/Ag ternary nanohybrid with improved visible light photocatalytic activity and stability. *Optik*. **217**, 164867, **2020**.
24. MACHOVSKY M., KURITKA I., KOZAKOVA Z. Microwave assisted synthesis of nanostructured Fe<sub>2</sub>O<sub>3</sub>/ZnO microparticles. *Materials Letters*, **86**, 136, **2012**.
25. RAMOS-DELGADO N., HINOJOSA-REYES L., GUZMAN-MAR I., GRACIA-PINILLA M., HERNÁNDEZ-RAMÍREZ A. Synthesis by sol-gel of WO<sub>3</sub>/TiO<sub>2</sub> for solar photocatalytic degradation of malathion pesticide. *Catalysis Today*, **209**, 35, **2013**.
26. LV K., LI J., QING X., LI W., CHEN Q. Synthesis and photo-degradation application of WO<sub>3</sub>/TiO<sub>2</sub> hollow spheres. *Journal of Hazardous Materials*, **189**, 329, **2011**.
27. ARTIOLI G. Science for the cultural heritage: the contribution of X-ray diffraction. *Rendiconti Lincei*, **24** (1), 55, **2013**.
28. TOMCZAK E., TOSIK P. Sorption Equilibrium of Azo Dyes Direct Orange 26 and Reactive Blue 81 onto a Cheap Plant Sorbent/Równowaga Sorpcji Barwników Azowych Direct Orange 26 I Reactive Blue 81 Na Tanim Sorbencie Roślinnym. *Ecological Chemistry and Engineering S.*, **21** (3), 435, **2014**.
29. ÖZBELGE T., EROL F., ÖNDER ÖZBELGE H. A kinetic study on the decolorization of aqueous solutions of Acid Red-151 by ozonation. *Journal of Environmental Science and Health, Part A.*, **38** (8), 1597, **2003**.
30. HASHEMIAN S. Removal of Acid Red 151 from water by adsorption onto nano-composite MnFe<sub>2</sub>O<sub>4</sub>/kaolin. *Main Group Chemistry*, **10** (2), 105, **2011**.
31. BASKARALINGAM P., PULIKESI M., ELANGO D., RAMAMURTHI V., SIVANESAN S. Adsorption of acid dye onto organobentonite. *Journal of Hazardous Materials*, **128** (2-3), 138, **2006**.
32. TEH P., PRAMANA S.S., KIM C., CHEN C., CHUANG C., SHARMA Y., CABANA J., MADHAVI

- S. Electrochemical Reactivity with Lithium of Spinel-type  $\text{ZnFe}_{2-y}\text{Cr}_y\text{O}_4$  ( $0 \leq y \leq 2$ ). *The Journal of Physical Chemistry C.*, **117** (46), 24213, **2013**.
33. WU W., ZHANG S., XIAO X., ZHOU J., REN F., SUN L., JIANG C. Controllable synthesis, magnetic properties, and enhanced photocatalytic activity of spindlelike mesoporous  $\alpha\text{-Fe}_2\text{O}_3/\text{ZnO}$  core-shell heterostructures. *ACS applied materials & interfaces*, **4** (7), 3602, **2012**.
34. DAVARI N., FARHADIAN M., NAZAR A.R.S., HOMAYOONFAL M. Degradation of diphenhydramine by the photocatalysts of  $\text{ZnO}/\text{Fe}_2\text{O}_3$  and  $\text{TiO}_2/\text{Fe}_2\text{O}_3$  based on clinoptilolite: Structural and operational comparison. *Journal of environmental chemical engineering*, **5** (6) 5707, **2017**.
35. WANG C., HUANG Z. Controlled synthesis of  $\alpha\text{-Fe}_2\text{O}_3$  nanostructures for efficient photocatalysis. *Materials Letters*, **164**, 194, **2016**.
36. MOMMA K., IZUMI F. VESTA: a three-dimensional visualization system for electronic and structural analysis. *Journal of Applied Crystallography*, **41**, 653, **2008**.
37. DAVARI N., FARHADIAN M., NAZAR A.R.S., HOMAYOONFAL M. Degradation of diphenhydramine by the photocatalysts of  $\text{ZnO}/\text{Fe}_2\text{O}_3$  and  $\text{TiO}_2/\text{Fe}_2\text{O}_3$  based on clinoptilolite: Structural and operational comparison. *Journal of environmental chemical engineering*, **5**, 6, **2017**.

